Prediction of Slot-Size and Inserted Air-Gap for Improving the Performance of Rectangular Microstrip Antennas Using Artificial Neural Networks

Taimoor Khan, *Member, IEEE*, Asok De, *Senior Member, IEEE*, and Moin Uddin, *Senior Member, IEEE*

***Abstract*—Artificial neural networks have been getting popularity for predicting various performance parameters of microstrip antennas due to their learning and generalization features. In this letter, a neural-networks-based synthesis model is presented for predicting the "*slot-size*" on the radiating patch and inserted "*air-gap*" between the ground plane and the substrate sheet, simultaneously. Different performance parameters like resonance frequencies, gains, directivities, antenna efficiencies, and radiation efficiencies for dual resonance are observed by varying the dimensions of slot and inserted air-gap. For validation, a prototype of microstrip antenna is fabricated using Roger's substrate, and its performance parameters are measured. Measured results show a very good agreement to their predicted and simulated values.**

***Index Terms*—Cross-slotted geometry, inserted air-gap, neural networks, rectangular microstrip patch, slot-size, synthesis model.**

I. Introduction

MICROSTRIP antennas (MSAs) are proved to be excellent radiators in different arenas of wireless communications like satellite communication, radar communication, global positioning system (GPS), and many more applications. Because of their operation in dual-frequency mode, the MSAs have eliminated two single-frequency operated antennas in these applications. In spite of having many attractive features like low profile, conformability to planar and nonplanar surfaces, low fabrication cost, etc., the MSAs suffer from the drawbacks of poor radiation characteristics (narrow bandwidth, low gain, low efficiency, etc.), which require more attention [1]. Different researchers have proposed different techniques for designing the MSAs for dual resonance such as multilayered stacked patch [2], [3], slotted rectangular patch [4], square patch with notches [5], patch loaded with shorting posts [6] or varactor diodes [7], and rectangular patch fed by an inclined slot [8]. These techniques [2]–[8] can be divided into analytical methods and numerical methods. The analytical methods offer comprehensive details for the operation of MSAs and are based on the physical assumptions for simplifying the radiating phenomenon of the MSAs. For this, such approaches are not suitable for the MSAs in which the thickness of the substrate is not very thin. On the other hand, the numerical methods provide fairly good results, but only at the cost of mathematical burden in the form of complex integral equations. The choice of test functions and path integrations emerge to be more significant without initial assumptions in the final stage of the numerical results. Also, these approaches require a new solution even for a very small change in the geometry. Thus, the obligation for having a new solution for every minor change in the geometry and the problems associated with the thickness of the substrates in analytical methods lead to complexities and processing cost [9].

In last decade, artificial neural network (ANN) models have acquired remarkable importance in wireless communications. It is so because of the ability and adaptability to learn and generalization features of the ANNs [9]–[12]. The ANN model can be trained by measured, calculated, and/or simulated samples. The purpose of training an ANN model is to minimize the error between the reference and the actual output of the ANN model. The trained neural model predicts the results very quickly for every small variation in the geometry both for electrically thin and thick MSAs. Different ANN models [13]–[20] have been proposed for analyzing and/or synthesizing the conventional MSAs. Few neural models [21]–[23] have been proposed for synthesizing the slotted MSAs. A synthesis modeling using ANN for predicting the size of truncated corners of square patch MSAs has been suggested by Wang *et al.* [24]. Robustillo *et al.* [25] have designed a contoured-beam reflectarray for a EuTELSAT European Coverage using ANN. An ANN modeling has been suggested by Freni *et al.* for modeling the behavior of the reflectarray reradiating elements [26]. In the literature [10]–[26], a neural-networks-based synthesis model has not been proposed for predicting the appropriate size of introduced slot on the radiating patch and inserted air-gap between the ground plane and the substrate sheet, simultaneously. It is very much essential for the antenna designers to predict the "*slot-size*" and inserted "*air-gap*" for achieving the desired level of performance parameters like 1.5 GHz $\leq$ *resonance frequencies* $\leq$3.0 GHz, 6.2 dBi $\leq$ *gains* $\leq$9.6 dBi, 6.6 dBi $\leq$ *directivities* $\leq$9.9 dBi, 83% $\leq$ *antenna efficiencies* $\leq$100%, and 85% $\leq$ *radiation efficiencies* $\leq$100% for dual-resonance. For this purpose, a simple and innovative neural-networks-based synthesis modeling is proposed in this letter.

Section II describes the geometry for samples generation. The neural-networks-based synthesis model is discussed in

Manuscript received September 05, 2013; accepted October 03, 2013. Date of publication October 10, 2013; date of current version October 24, 2013.

The authors are with the Department of Electronics and Communication Engineering, Delhi Technological University, Delhi 110 042, India (e-mail: ktaimoor@gmail.com).

Color versions of one or more of the figures in this letter are available online at http://ieeexplore.ieee.org.

Digital Object Identifier 10.1109/LAWP.2013.2285381

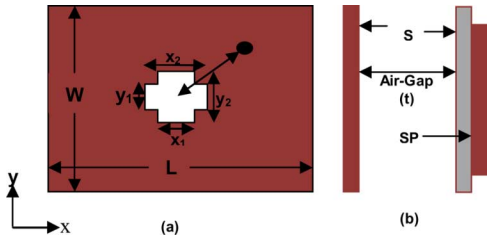

Fig. 1. Proposed antenna. (a) Top view. (b) Side view.

Section III. Section IV illustrates the experimental results and discussion. A conclusion is discussed in Section V.

II. Proposed Geometry for Samples Generation

The cross-sectional view of the proposed antenna is shown in Fig. 1, in which the terms GP, S, and SP represent ground plane, substrate, and slotted patch, respectively.

Here a rectangular patch of dimensions 61×56 mm^2 is used with a ground plane of dimensions 200×175 mm^2. The antenna is simulated in method of moments (MoM)-based IE3D software [27] using RT-Duroid substrate RO3003 ($\varepsilon_r = 3, h = 0.762$ mm, and $\tan\delta = 0.0045$) for dual resonance. The proposed antenna is excited by a single probe. A total of 1350 samples for dual resonance (*DR*), dual-frequency gain (*DFG*), dual-frequency directivity (*DFD*), dual-frequency antenna efficiency (*DFA*), and dual-frequency radiation efficiency (*DFR*) are generated by varying the slot-size between 1 mm $\leq$ slot-size $\leq$ 50 mm and inserted air-gap between 1 mm $\leq$ air-gap $\leq$10 mm, simultaneously. These samples are generated in IE3D software on a computer system with the following system configuration: Dell Optiplex 780 Core 2 Duo CPU E8400, 3.0 GHz with 4.0 GB RAM. These generated samples are used for training as well as testing of the proposed neural networks model, which is to be discussed in Section III.

III. Neural Network Modeling

ANNs are becoming powerful techniques for obtaining solutions to the problems that are cross-disciplinary in nature. The neural networks are extremely distributed analogous processors that have usual tendency for storing the empirical knowledge during training and making it available for use during testing. ANN models resemble the brain since knowledge is acquired by the neural networks through a training process, and interneuron connection strengths are used to store that knowledge [9]. Few known examples of a problem are used to acquire this knowledge during training of the ANN model. The trained model is then set to use this acquired knowledge effectively in solving "unknown" or "untrained" instances of the problems [9]. Multilayered perceptron (MLP) neural networks consist of an input layer, a hidden layer (or a number of hidden layers), and an output layer. Each layer in the model has an entirely different role. Three common steps are used to train the MLP neural networks. First, the training samples are generated, the structural configuration of the hidden layer is then selected in the second step, and finally, in the third step, the weights and biases are optimized using training algorithm. The trained ANN model is then tested on an arbitrary sets of samples that are not included in the training samples. Coding for training and testing algorithms of the ANN model is created in MATLAB software [28].

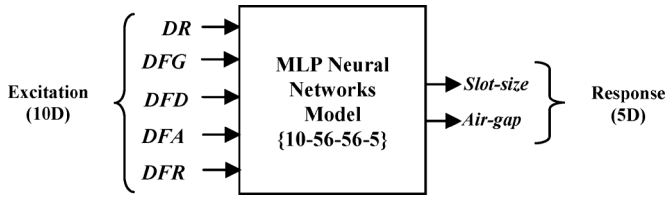

Fig. 2. Synthesis MLP neural model.

TABLE I
Sampling of Slot-Size and Inserted Air-Gap

Sampling of Slot-Size and Air-Gap			Generated Samples
Slot-Size	**Specified Range**	**Step-Size**	
x_1	$1\text{mm} \leq x_1 \leq 50\text{mm}$	36μm	For Training= 1000 Nos.
y_1	$1\text{mm} \leq y_1 \leq 50\text{mm}$	36μm	For Testing = 350 Nos.
x_2	$1\text{mm} \leq x_2 \leq 50\text{mm}$	36μm	
y_2	$1\text{mm} \leq y_2 \leq 50\text{mm}$	36μm	
Air-Gap	**Specified Range**	**Step-Size**	
t	$1\text{mm} \leq t \leq 10\text{mm}$	7μm	

A. Training and Testing Samples Generation

It is a common fact that the neural networks model, trained on a set of samples (known as training samples), produces results very fast. However, generation of samples and allocating them into training and testing samples is a challenging task for a complicated geometry where excitation-response is multidimensional. In Section II, a total of 1350 samples are generated by varying the slot-size (x_1, y_1, x_2, and y_2) and inserted air-gap (t) for the geometry shown in Fig. 1. The sampling used for creating these samples is shown in Table I. Different performance parameters like resonance frequencies (f_1 and f_2), gains (G_1 and G_2), directivities (D_1 and D_2), antenna efficiencies (A_1 and A_2), and radiation efficiencies (R_1 and R_2) for dual resonance are observed by varying the slot-size and air-gap. Hence, a 10-dimensional response matrix is achieved by varying the five-dimensional excitation matrix. For ANN modeling, a reverse strategy is used for predicting the five-dimensional geometrical parameters $[r] \rightarrow [x_1\ y_1\ x_2\ y_2\ t]$ for the given 10-dimensional performance parameters $[x] \rightarrow [f_1\ f_2\ G_1\ G_2\ D_1\ D_2\ A_1\ A_2\ R_1\ R_2]$.

B. Proposed Structure of the Neural Model and Training Algorithms

An ANN model for predicting the "*slot-size*" and inserted "*air-gap*" is shown in Fig. 2.

Training of an ANN model basically consists of adjusting weights and biases for the applied input sample to get the desired response. This adjustment is carried out by using a training algorithm. The training performance is observed by varying the number of hidden layers as well as the neurons in each hidden layer. After several trials, the structural configuration of the model is optimized as {10-56-56-5} for the best performance. It means that there are 10 neurons in the input layer, 56 neurons each in first and second hidden layer, and five neurons in the output layer. Furthermore, the training performance of the model is observed for seven different algorithms: BFGS quasi-Newton (BFG), Bayesian regulation (BR),

TABLE II
PERFORMANCE OF PROPOSED ANN MODEL

Algo.	Average Absolute Error during Training of ANN		Average Absolute Error during Testing of ANN		Training Time	Iteration Required
	Slot-Size	Air-Gap	Slot-Size	Air-Gap		
BFG	23.29 mm	13.41 mm	30.12 mm	39.44 mm	3467 sec.	79342
BR	16.25 mm	23.23 mm	27.53 mm	36.36 mm	3269 sec.	72391
SCG	25.46 mm	19.21 mm	29.40 mm	35.49 mm	5392 sec.	76184
CGB	17.59 mm	20.12 mm	25.12 mm	37.18 mm	2485 sec.	76734
CGF	16.04 mm	22.88 mm	29.38 mm	29.41 mm	7226 sec.	78832
OSS	21.41 mm	19.65 mm	24.66 mm	33.39 mm	5638 sec.	83136
LM	**7.18 mm**	**6.99 mm**	**9.96 mm**	**8.47 mm**	**1307 sec.**	**31739**

scaled conjugate gradient (SCG), Powell–Beale conjugate gradient (CGB), conjugate gradient with Fletcher-Peeves (CGF), one-step secant (OSS), and Levenberg–Marquardt (LM), respectively [29]. The samples generated in IE3D simulator are normalized between +0.1 to +0.9 in MATLAB software before applying training. For an applied input pattern, the arbitrary numbers between 0 and 1 are assigned to initialize the weights and biases. The output of the model is then calculated for that input pattern. The mean square error (MSE) between the predicted and the simulated outcomes is also computed, and the weights and biases are then updated accordingly. This updating process is carried out after presenting each set of input sample until the calculated accuracy of the model is estimated satisfactory for 1000 training samples. Training of the model is done by taking some initial parameters: $\text{MSE} = 3.45 \times 10^{-6}$, *learning rate* $(\eta) = 0.631$, and *momentum coefficient* $(\mu) = 0.518$.

The testing algorithm is then realized for the remaining 350 samples. For this realization, all the initial weights and biases are replaced by their corresponding optimized values. The trained model then predicts the "*slot-size*" introduced on the radiating patch and the inserted "*air-gap*" between the ground plane and the substrate sheet, simultaneously within a fraction of a second for any arbitrary set of resonance frequencies, gains, directivities, antenna efficiencies, and radiation efficiencies for dual resonance within their specified ranges mentioned in Section I.

IV. Experimental Results and Discussion

The training performance of the ANN model discussed in Section III is observed for seven different algorithms; BFG, BR, SCG, CGB, CGF, OSS, and LM algorithms, respectively. The average absolute error in predicting the "*slot-size*" and inserted "*air-gap*" both for training and testing of the model is mentioned in Table II. The time elapsed in training of the model for each algorithm is specified in the sixth column of Table II, whereas the number of iterations required is in the seventh column of the table. Hence, the LM algorithm is proved to be the most accurate training algorithm for the proposed problem as it produces the least error both for training and testing of the model. It is also proved to be the fastest training algorithm as it requires the least training time (1307 s) and minimum number of iterations (31 739) during training of the ANN model.

The weights and biases for the proposed neural model are selected randomly for initialization. Hence, the stochastic behavior (mean and standard deviation) of the five-dimensional absolute error corresponding to five-dimensional response is also calculated. The mean is the sum of the observations divided by the number of observations and identifies the central location of the error set. The standard deviation is the most common measure of variability, measuring the spread of the error set and the relationship of the mean to the rest of the error. The error points closer to the mean indicate fairly uniform responses with small value of the standard deviation. Conversely, the error points far from the mean show a wide variance in the response and large value of the standard deviation. Another term, i.e., coefficient of variation (CoV), is also defined to know the relationship between the mean and the standard deviation of an error set. It is defined as the ratio of standard deviation to the mean value. CoV closer to 0 represents greater uniformity of error, whereas CoV closer to 1 represents the large variability of the error. For LM algorithm, the means for five-dimensional errors are computed as 1.5061, 1.4927, 1.5217, 1.4956, and 1.4932, respectively, whereas their corresponding standard deviations are found as 0.2910, 0.3062, 0.2824, 0.3229, and 0.3033, respectively. Hence, the coefficients of variations for these five values are coming out to be 0.1932, 0.2051, 0.1856, 0.2159, and 0.2031, respectively. Thus, it is concluded here that all the error points over a full validation set of 1350 samples are uniformly distributed [26].

During simulation in IE3D software, 1.5–3.0 GHz frequency range with total 100 sampling points for each simulating structure is used, and a total 1350 such structures is simulated. The simulation time in the IE3D software depends on the complexity inserted in the geometry. For the proposed geometry, it is computed as ∼6700 s (or ∼1 h, 53 min) per structure. During each simulation, 36 MB system memory (RAM) is required. By using the ANN modeling, the computational time and the required memory storage is fairly reduced. The time elapsed during training of the ANN model is already computed as 1307 s (see Table II). The time elapsed during testing of the ANN model is computed in the MATLAB software on a computer system using MATLAB syntax "cputime" as follows:

$$\begin{gathered}\text{clc; clear all;}\\ \text{time\_1} = \text{cputime;}\\ \textit{Start of testing algorithm}\\ \textit{Program statement-1}\\ \textit{Program statement-2}\\ \cdots\cdots\cdots\cdots\cdots\cdots\cdots\cdots\cdots\cdots\\ \cdots\cdots\cdots\cdots\cdots\cdots\cdots\cdots\cdots\cdots\\ \textit{End of Testing Algorithm}\\ \text{Computational Time\_ANN} = \text{cputime-time\_1}\end{gathered}$$

This procedure is repeated for 350 independent runs and finally concludes that the ANN model requires ∼53 ms in producing the results after training. Thus, the neural approach after training is much faster than the simulation approach.

Furthermore, the training of the model requires only 29 kB RAM of a system and for testing the performance, only 1.4 kB RAM is required. Hence, the required memory space in training as well as testing of the model is also lesser as compared to 36 MB required for simulation.

For validating the work, a prototype is fabricated using RT-Duroid substrate. The patch of dimensions 61×56 mm^2 is etched on the upper side of the substrate, whereas an air-gap of 5.1 mm between the substrate and the ground plane is inserted

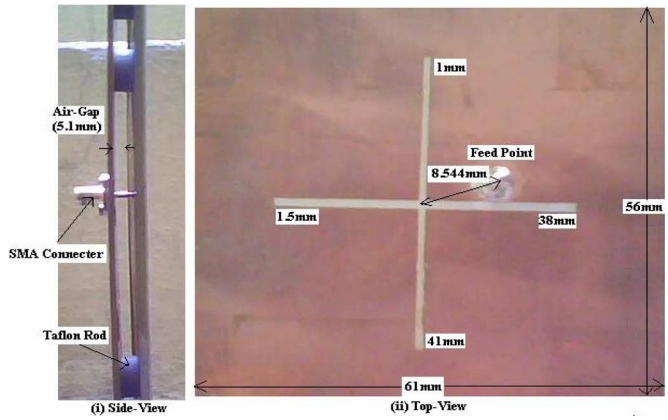

Fig. 3. Enlarged view of fabricated antenna.

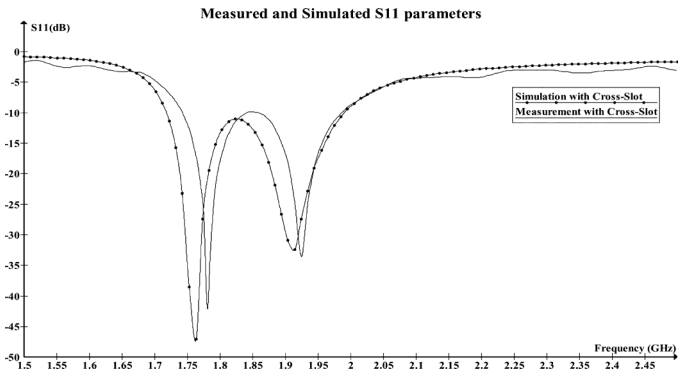

Fig. 4. Comparison of measured and simulated S-parameters.

TABLE III
COMPARISON OF SIMULATED AND PREDICTED RESULTS

Name of Parameter	Simulated value in IE3D	Predicted value using ANN
x_1 (mm)	38.0000	37.9209
y_1 (mm)	1.5000	1.5021
x_2 (mm)	1.0000	0.9567
y_2 (mm)	41.0000	41.0561
t (mm)	5.1000	5.1023

using Teflon rods (see Fig. 3). The prototype is excited by probe feed, which guides the electromagnetic waves to the feed point. An SMA connector with a 6.8-mm-long pin (1 mm for ground plane + 5.1 mm for air-gap + 0.762 mm for substrate) is used for RF connection. The S-parameters of the fabricated prototype are measured using Agilent N5230A network analyzer. A comparison between measured and simulated S-parameters is depicted in Fig. 4, which shows a good convergence between the two. It is also confirmed here that the Teflon rods do not affect the antenna performance. A comparison between simulated and predicted parameters for the fabricated prototype is given in Table III, which shows a good agreement between the two. A very good conformity is also achieved if the simulated dual resonance (DR) is compared to its measured counterparts as mentioned in Table IV.

Table V shows the improvement in the performance parameters by inserting the cross-slot on the patch antenna. By introducing the slot, the excited surface current path lengthens,

TABLE IV
COMPARISON OF SIMULATED AND MEASURED DR

Specifications of slot-size and inserted air-gap	Simulated DR in IE3D	Measured DR
Slot-size: $x_1 = 38.0$mm, $y_1 = 1.5$mm, $x_2 = 1.0$mm & $y_2 = 41.0$mm **Air-gap:** t = 5.1mm	1.7708 GHz and 1.9221 GHz	1.7800 GHz and 1.9250 GHz

TABLE V
IMPROVEMENT IN PERFORMANCE PARAMETERS

Performance Parameter	Without cross-slot	With cross-slot	Remarks
DR (GHz)	2.0256 and 2.1970	1.7630 and 1.9140	**Desired**
DFG (dBi)	8.2026 and 8.2129	8.9365 and 8.9387	**Desired**
DFD (dBi)	9.1428 and 9.4193	9.1122 and 9.2079	Un-desired
DFA (%)	80.5329 and 85.3708	95.8065 and 93.9897	**Desired**
DFR (%)	90.2454 and 93.7718	96.3604 and 96.6599	**Desired**

increasing the antenna length, hence decreasing the resonance frequency. For the case of slotted patch, both the resonance frequencies (1.763 and 1.914 GHz) are lowered by ~13% as compared to those (2.0256 and 2.1970 GHz) of the patch geometry without a slot, which can result to a patch size reduction of ~35% for a given dual-frequency design. Hence, a good rank of compactness is achieved in the fabricated prototype. Furthermore, the gains and efficiencies are also improved, but only at the cost of slight reduction in the directivities. The gain of an antenna is defined as the product of directivity and radiation efficiency. Hence, it is improved by increasing the radiation efficiencies.

A bandwidth of 55.5 MHz is achieved (see Fig. 4) for $S_{11} \leq -10$ dB during simulation, but it increases to 250 MHz (1.99–1.74 GHz) in the fabricated prototype during measurement. It may be probably due to irregularity in fabricating the prototype and/or inserting the air-gap using Teflon rods. Furthermore, the size and losses of the solder joints are not considered during the simulation, which may cause this difference between them.

The ratio (f_2/f_1) of the two frequencies is also computed as 1.0846 $(=2.1970/2.0256)$, 1.0857 $(=1.914/1.763)$, and 1.0815 $(=1.925/1.780)$ for the original geometry without any slot, simulated slotted geometry, and fabricated slotted prototype, respectively. Thus, the ratio (f_2/f_1) is slightly affected by inserting the cross-slot, and mainly determined by the aspect ratio $(1.89 = 61/56)$ of the patch; which makes the design simpler and easier to implement.

An extremely good impedance matching is also achieved by inserting the air-gap between the substrate sheet and the ground plane. Consequently, the antenna and radiation efficiencies both significantly are improved because of very small amount of dielectric loss in the air substrate.

V. CONCLUSION

In this letter, an accurate, simple, and fast ANN-based synthesis modeling scheme has been proposed to predict the required "slot-size" and inserted "air-gap" simultaneously in order to achieve desired level of radiation patterns of rectangular microstrip antennas. Such a neural approach is rarely proposed in the open literature to the best of our knowledge for the 10-dimensional excitation and five-dimensional response.

It takes only a fraction of a second in predicting the required results after doing training properly. The approach has produced more accurate results, hence it can also be recommended to include in antenna computer-aided design (CAD) algorithms.

The computational time and required system memory have been calculated and concluded that the neural approach requires a lesser amount of computational time and the system memory after training.

In general, computing five-dimensional response may require five different neural networks modules, whereas in the present work, only one module is fulfilling the requirement of five independent modules. During synthesis of the antenna, it is desirable for the design engineers to know different performance parameters of an antenna simultaneously, instead of knowing individual parameters, alternatively. Hence, the present approach has been considered more generalized and efficient.

For validation purpose, a prototype has also been fabricated. A very good convergence between measured and simulated results has been achieved, which supports the effectiveness of the proposed work.

REFERENCES

[1] I. J. Bahl and P. Bhartia, *Microstrip Antennas*. Dedham, MA, USA: Artech House, 1980.

[2] J. S. Dahele, K. F. Lee, and D. P. Wong, "Dual-frequency stacked annular-ring microstrip antennas," *IEEE Trans. Antennas Propag.*, vol. AP-35, no. 11, pp. 1281–1285, Nov. 1987.

[3] S. A. Long and M. D. Walton, "A dual-frequency stacked circular-disc antenna," *IEEE Trans. Antennas Propag.*, vol. AP-27, no. 2, pp. 270–273, Mar. 1979.

[4] S. Maci, G. B. Gentili, and G. Avitabile, "Single-layer dual-frequency patch antenna," *Electron. Lett.*, vol. 29, pp. 1441–1443, 1993.

[5] H. Nakano and K. Vichien, "Dual-frequency square patch antenna with rectangular notch," *Electron. Lett.*, vol. 25, pp. 1067–1068, 1989.

[6] D. H. Schaubert, F. G. Farrar, A. Sindoris, and S. T. Hayes, "Microstrip antennas with frequency agility and polarization diversity," *IEEE Trans. Antennas Propag.*, vol. AP-29, no. 1, pp. 118–123, Jan. 1981.

[7] R. B. Waterhouse and N. V. Shuley, "Dual-frequency microstrip rectangular patches," *Electron. Lett.*, vol. 28, 1992.

[8] Y. M. M. Antar, A. I. Ittipiboon, and A. K. Bhattacharyya, "A dual-frequency antenna using a single patch and an inclined slot," *Microw. Opt. Technol. Lett.*, vol. 8, pp. 309–311, 1995.

[9] Q. J. Zhang and K. C. Gupta, *Neural Networks for RF and Microwave Design*. Norwood, MA, USA: Artech House, 2000.

[10] P. M. Watson and K. C. Gupta, "EM-ANN models for microstrip vias and interconnects in dataset circuits," *IEEE Trans. Microw. Theory Tech.*, vol. 44, no. 12, pp. 2495–2503, Dec. 1996.

[11] P. M. Watson and K. C. Gupta, "Design and optimization of CPW circuits using EM-ANN models for CPW components," *IEEE Trans. Microw. Theory Tech.*, vol. 45, no. 12, pp. 2515–2523, Dec. 1997.

[12] P. M. Watson, K. C. Gupta, and R. L. Mahajan, "Development of knowledge based artificial neural network models for microwave components," in *Proc. IEEE MTT-S Int. Microw. Symp. Dig.*, 1998, vol. 1, pp. 9–12.

[13] D. Karaboga, K. Guney, S. Sagiroglu, and M. Erler, "Neural computation of resonance frequency of electrically thin and thick rectangular microstrip antennas," *Inst. Elect. Eng. Proc., Microw., Antennas Propag.*, vol. 146, pp. 155–159, 1999.

[14] S. Sagiroglu, K. Guney, and M. Erler, "Resonant frequency calculation for circular microstrip antennas using artificial neural networks," *Int. J. RF, Microw. CAE*, vol. 8, pp. 270–277, 1998.

[15] S. Sagiroglu and K. Guney, "Calculation of resonant frequency for an equilateral triangular microstrip antenna with the use of artificial neural networks," *Microw. Opt. Technol. Lett.*, vol. 14, pp. 89–93, 1997.

[16] R. Gopalakrishnan and N. Gunasekaran, "Design of equilateral triangular microstrip antennas using artificial neural networks," in *Proc. IEEE IWAT*, 2005, pp. 246–249.

[17] K. Guney, S. Sagiroglu, and M. Erler, "Generalized neural method to determine resonant frequencies of various microstrip antennas," *Int. J. RF Microw. CAE*, vol. 12, pp. 131–139, 2002.

[18] K. Guney and N. Sarikaya, "A hybrid method based on combining artificial neural network and fuzzy inference system for simultaneous computation of resonant frequencies of rectangular, circular, and triangular microstrip antennas," *IEEE Trans. Antenna Propag.*, vol. 55, no. 3, pp. 659–668, Mar. 2007.

[19] K. Guney and N. Sarikaya, "Concurrent neuro-fuzzy systems for resonant frequency computation of rectangular, circular, and triangular microstrip antennas," *Prog. Electromagn. Res.*, vol. 84, pp. 253–277, 2008.

[20] N. Turker, F. Gunes, and T. Yildirim, "Artificial neural design of microstrip antennas," *Turk. J. Elec. Eng.*, vol. 14, pp. 445–453, 2006.

[21] D. K. Neog, S. S. Pattnaik, D. C. Panda, S. Devi, B. Khuntia, and M. Dutta, "Design of a wideband microstrip antenna and the use of artificial neural networks in parameter calculation," *IEEE Antennas Propag. Mag.*, vol. 47, no. 3, pp. 60–65, Jun. 2005.

[22] V. V. Thakare and P. K. Singhal, "Bandwidth analysis by introducing slots in microstrip antenna design using ANN," *Prog. Electromagn. Res. M*, vol. 9, pp. 107–122, 2009.

[23] V. V. Thakare and P. Singhal, "Microstrip antenna design using artificial neural networks," *Int. J. RF Microw. CAE*, vol. 20, pp. 76–86, 2010.

[24] Z. Wang, S. Fang, Q. Wang, and H. Liu, "An ANN-based synthesis model for the single-feed circularly-polarized square microstrip antenna with truncated corners," *IEEE Trans. Antennas Propag.*, vol. 60, no. 12, pp. 5989–5992, Dec. 2012.

[25] P. Robustillo, J. Zapata, J. A. Encinar, and M. Arrebola, "Design of a contoured-beam reflectarray for a EuTELSAT European coverage using a stacked-patch element characterized by an artificial neural network," *IEEE Antennas Wireless Propag. Lett.*, vol. 11, pp. 977–980, 2012.

[26] A. Freni, M. Mussetta, and P. Pirinoli, "Neural network characterization of reflectarray antennas," *Int. J. Antennas Propag.*, vol. 2012, pp. 541354-1–541354-10, 2012.

[27] IE3D. ver. 14.0, Zeland Software, Inc., Fremont, CA, USA, Oct. 2007.

[28] D. J. Higham and N. J. Higham, *MATLAB Guide*. Philadelphia, PA, USA: SIAM, 2005.

[29] M. T. Hagan and M. B. Menhaj, "Training feedforward networks with the Marquardt algorithm," *IEEE Trans. Neural Netw.*, vol. 5, no. 6, pp. 989–993, Nov. 1994.